This full-text paper was peer-reviewed and accepted to be presented at the IEEE WiSPNET 2017 conference.

A Covariance-Convolution Framework for Radar Intra-Pulse Modulation Classification

A.R. Sachin,[1] Hemant V. Paranjape[2] and K. Maheswara Reddy[3]
Defence Avionics Research Establishment, Defence Research and Development Organisation
Ministry of Defence, Government of India, Bangalore-560093, Karnataka, India.
Email: [1]sachin@dare.drdo.in [2]hemant@dare.drdo.in [3]maheswara@dare.drdo.in

***Abstract*—In this paper, a signal processing algorithm for modulation classification of pulse-compressed threat radar signals by an airborne, electronic warfare (EW) digital receiver (DRx) is presented. Modern radars employ pulse compression techniques like frequency modulation (FM), phasemodulation (PM), frequency hopping (FH), etc. to achieve specific operational objectives. State-of-the-art technologies and systems enable broadband signal design, intra-pulse techniques and joint-domain analysis in radars. To counter modern radars, EW systems need to have real-time adaptive capabilities, in multiple domains, over the vast multi-parametric space of radar operations. Current work focusses on the challenges associated with intra-pulse modulation classification, pivotal for scenario cognition. Novelty of the proposed method is itsapplicability for analysis of arbitrary intra-pulse techniques, by treating pulse compression as continuous time (CT) or discrete time (DT) process and classification based on the underlying signal structure. The method is a two-level classifier designed for four classes of signals viz. Unmodulated (Unmod), FM, PM and FH. In the first level, classification is done between CT and DT modulations. By design, Unmod & FM are CT modulations, while PM & FH are DT modulations. In the second level, classification is done between Unmod & FM and between PM & FH. The method utilizes covariance, convolution and stationarity properties of signals of interest. Classification performance in multi-parametric space of each modulation type, is quantified in terms of confusion probabilities over SNR. Efficacy of proposed method has been ascertained in the actual EW DRx, against signals generated using radar signal design library & advanced signal generators.**

***Index Terms*—Barker Code, Costas Code, Electronic Warfare, Frank Code, Pearson Correlation Coefficient, Pulse Compression.**

I. Introduction

Pulse compressed radars are strategic force-multipliers with operational advantages like longer range-to-target, fine range resolution, low peak power, etc. [1]. These techniques are pivotal in achieving covertness and electronic counter counter measures against electronic warfare (EW) systems [2]. To be relevant in modern electronic battlefield, EW systems need to have competitive design and operational philosophy. It is imperative that, real time interception and classification in dense threat scenarios is crucial for platform survivability. To illustrate the significance of intra-pulse analysis, consider a radar signal with 1 μS pulse width (PW), designed for 150 m range resolution. A 13-bit Barker or a 8×8 Frank coded signal achieve the same resolution with 13 μS and 64 μS PWs respectively. Longer PWs can be used either to achieve longer range or covertness by reduced peak power. A linear frequency modulated (LFM) signal with 200 MHz bandwidth (BW) has 0.75 m range resolution with longer PW & low peak power, while an unmodulated signal needs 5 nS PW with large peak power for equivalent performance. Reliable, real-time & accurate threat classification is essential for effective EW battlefield adaptations in time, spectral & spatial domains.

Commercially, prominent Radar and EW system manufacturers like [3–6] specify intra-pulse analysis as a prominent feature in modern EW systems. Pioneering work has been done by Pace in [2], which is one of the most comprehensive literature on the subject. Extensive research work based on artificial neural networks is reported in [7]. Spectrogram, Wigner-Ville & Choi-Williams distributions have been successfully used for signal analysis in [8]. An interesting method using Short-Time Harmonic Model and Kolmogorov-Smirnov test is presented in [9]. Authors have proposed a comprehensive solution for detection, characterization and geo-localization. Design aspects of low probability of recognition radars and its performance as a function of covertness is holistically presented in [10]. A highly accurate classification method, based on modulation component analysis and instantaneous frequency rate is presented in [11]. A novel radar emitter recognition approach based on three-dimensional distribution feature and transfer learning is proposed in [12]. A comprehensive method based on Nyquist folding receiver concept is proposed in [13], for parameter estimation of hybrid LFM/BPSK signals.

Current work is based on analysis of frequency/phase stationarity of signals. An introduction to frequency modulation (FM), phase modulation (PM) and frequency hopping (FH), is presented in Section II. Section III outlines the objectives and scope of current work. Section IV presents problem statement and the proposed solution along with the Algorithm, in mathematical form. System implementation, performance analysis and conclusion are presented in Sections V–VII respectively.

Notations: Bold lower case Roman letters denote vectors. $\mathbf{x}$ is a column vector. $\mathbf{x}_{\{i,k\}}$ is the ith frame of $\mathbf{x}$ formed by kth index set. $\hat{F}$ denote estimate of F. $\mathcal{P}$ denote probability. $\|.\|$ denote vector 2-norm. $\sim$ denote 'distributed as'. $\mathcal{N}$

978-1-5090-4442-9/17/$31.00

and $\mathcal{U}$ denote Normal and Uniform distributions respectively. $\mathbb{PCC}\{\mathbf{x},\mathbf{y}\}$ denote Pearson correlation coeffecient of $\mathbf{x}$ and $\mathbf{y}$. $\mathbb{DFT}\{\mathbf{x},N\}$ & $\mathbb{IDFT}\{\mathbf{x},N\}$ denote N-point Fourier Transform and inverse Fourier Transform of $\mathbf{x}$ respectively.

II. Intra Pulse Modulations

A. Frequency Modulation

FM signals have continuous instantaneous frequency (IF) & can be represented by qth order polynomial. LFM is a widely used pulse compression technique due to a host of advantages. Respective expressions for generic FM & LFM are as below.

$$s[n] = (\alpha)\exp\left\{j\left[\left(\omega_0 n + \omega_1 n^2 + \ldots + \omega_q n^{q+1}\right) + \varphi\right]\right\} \tag{1}$$

$$s[n] = (\alpha)\exp\left\{j\left[2\pi\left(\left(F \mp \frac{B}{2}\right)n \pm \frac{B}{2T}n^2\right) + \varphi\right]\right\} \tag{2}$$

where $j = \sqrt{-1}$, $\mathbf{s}$: Signal vector, α: Magnitude, φ: Initial phase offset, n: Time index, q: Polynomial order, ω_i: Parametric coefficients, F: Center frequency, B: Modulation bandwidth and T: Modulation period.

Polynomial orders, $q = 0$ & $q = 2$ represent unmodulated & quadratic FM respectively. FMCW radar signals have periodic IF with unique positive & negative slopes and each unidirectional slope represented by (1). In FM radars, range resolution is inversely proportional to signal bandwidth.

B. Phase Modulation

PM signals have constant amplitude, continuous wave (CW) structure with discrete phase change patterns over the pulse. Each phase state is maintained over a defined chip width, which determines the achievable range resolution. PM may be bi-phase or poly-phase and can be expressed as below.

$$s[n] = (\alpha)\exp\left\{j[\omega n^{\{k\}} + \varphi_k]\right\} \tag{3}$$

where φ_k & $\{n^{\{k\}}\}$ denote phase & time vector for kth chip. Barker codes are prominent among bi-phase codes and are known for excellent side lobe performance in radars. Among poly phase techniques, P_1, P_2, P_3, P_4 and Frank codes are widely employed for pulse compression. Detailed discussion on various bi-phase and poly-phase codes can be found in [2].

C. Frequency Hopping

FH is basically discrete step FM within the pulse, imparting significant operational advantages to radars. FH builds high uncertainty in time-frequency domain of the signal, lowering its probability of interception. Generic expression for FH is as below.

$$s[n] = (\alpha)\exp\left\{j[\omega_k n^{\{k\}} + \varphi]\right\} \tag{4}$$

where ω_k & $\{n^{\{k\}}\}$ denote frequency & time vector for kth sub pulse. FH may have arbitrary number of hops, with definite or random hop sequence and equal or unequal PW. Special FH patterns like Costas code are designed to achieve specific range resolution, broad bandwidth & anti-jamming properties.

III. Objectives and Scope

A. Objectives

To develop an algorithm for the intra-pulse modulation classification among four classes of interest viz. Unmod, PM, FM and FH comprising sub classes as enumerated below.

- PM: Barker, Frank, P_n, Bi-phase & Poly-phase codes
- FM: Linear/Non linear FM, FMCW, Arbitrary FM
- FH: Definite/random hops with equal/unequal sub PWs.

B. Scope

- Distinction among sub classes within a specific modulation class is beyond the scope of current work
- If a continuous time (CT) process has discrete time (DT) event(s) embedded, the same is classified as DT process.

IV. Problem Statement and Proposed Solution

Received real process, $\mathbf{b}_r$ is a linear combination of signal of interest (SOI) & additive white gaussian noise (AWGN).

$$\mathbf{b_r}_{L\times 1} = \mathbf{s}_r + \mathbf{w}_r, \qquad \mathbf{w}_r \sim \mathcal{N}(\mathbf{0}, \sigma^2\mathbf{I}_L) \tag{5}$$

where $\mathbf{s}_r$ has specific structure depending on signal & modulation parameters. Under the current scope, there are four hypotheses. The problem is to detect defining structure of modulation types by observing SOI response to specific signal processing functions, define decision framework based on classifier metrics and develop work flow for implementation.

Proposed solution is based on covariance, convolution and stationarity properties of the SOIs. By definition, Unmod signal has constant frequency and continuous phase. FM signal has time varying frequency and continuous phase. These properties allow modelling of Unmod and FM as CT processes. PM and FH signals have constant frequency and continous phase over the chips/sub pulses, and are characterized by discrete phase change and discrete frequency change events respectively. Within a chip/sub PW, PM and FH are essentially Unmod signals. This qualifies PM and FH as DT processes.

Proposed solution, presented in **Algorithm 1**, is designed from a system perspective. Input comprises SOI sample vector, a threshold-set, specific to system and an index-set, specific to processing architecture. Complex covariance and convolution are implemented in spectral domain based on Wiener-Khinchin Theorem and Hilbert Transform [14]. Analytical derivations for thresholds & indices require dedicated space for discussion. In this paper, role of thresholds & indices in setting parametric bounds, trade-offs & achievable performance is discussed.

In the first level, complex convolution of $\mathbf{b_r}$ is computed in $(M_1 \times 1)$ frames over the PW. Pearson correlation coefficient (PCC) of the complex convolution vector & its flipped version is computed for each frame. Due to stationarity of CT SOIs over M_1 samples, vector $\mathbf{u}$ is highly correlated to its flipped version. For DT cases, frames with discrete events show loss of correlation as a function of lag position of the event. Discrete event propagates in steps of m_1 samples, with choice of m_1 ensuring capture of lowest PCC value. $P_{Th}^{\{1\}}$ depends on minimum phase change & minimum hop, intended to

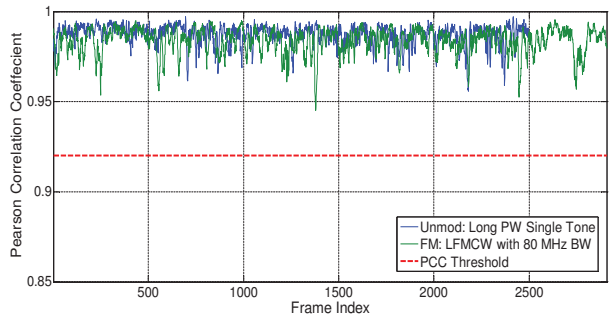

Fig. 1. Continuous-time process classification: Pearson correlation coefficient vector plots for Unmod & FM signals. $P_{Th}^{\{1\}} = 0.92$. SNR $= 4$ dB.

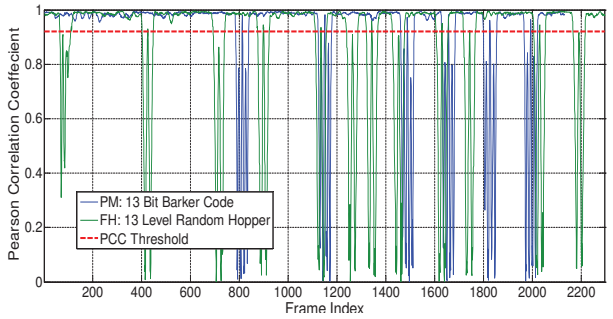

Fig. 2. Discrete-time process classification: Pearson correlation coefficient vector plots for PM & FH signals. $P_{Th}^{\{1\}} = 0.92$. SNR $= 4$ dB.

be detected and on maximum BW over M_1 samples for FM. Even a single threshold crossing event result in DT classification. Framewise PCC analysis continues for N_{DT} threshold crossing events in case of DT & N frames for CT.

If classified as CT, FM is distinguished based on frequency non-stationarity over longer durations of time. Covariance and convolution vectors, $\mathbf{v}_1$ & $\mathbf{v}_2$, over M_3 samples ($M_3 > M_1$) and corresponding PCC are computed. $P_{Th}^{\{2\}}$ and M_3 are chosen based on minimum FM BW to be classified and maximum correlation loss for Unmod signals at cut off SNR.

If classified as DT, individual chips for PM and sub pulses for FH are extracted based on event marking and corresponding N_{DT} frequencies are computed using high resolution, M_2-point DFT. For PM, all chips are of same frequency and hence can be separated from FH using B_{Th} thresholding.

V. System Implementation

Proposed algorithm is integrated in the system software of DRx, as intra-pulse analysis library. Algorithm is initiated after pulse extraction by detector/extractor module. Based on classification, analysis proceeds to the relevant estimator module. Firstly, functioning of the algorithm on typical modulation cases is illustrated. Fig. 1 for Unmod & FM cases show that PCC is centered around 0.985, with its minima $> P_{Th}^{\{1\}}$ at 4 dB SNR. Above 6 dB SNR, PCC vector is tightly bounded near unity, for the parametric space considered. Fig. 2 for PM & FH show $P_{Th}^{\{1\}}$ crossings at every DT event in SOI & PCC concentration well above $P_{Th}^{\{1\}}$ in between the events.

Algorithm 1 Intra-Pulse Modulation Classifier

Inputs: $\mathbf{b}_{\mathbf{r}L\times1}, L, \{P_{Th}^{\{1\}}, P_{Th}^{\{2\}}, T_{Th}, B_{Th}, N, N_{CT}, N_{DT}\}$ $\{M_1, M_2, M_3, m_1, m_2, m_3\}$.
Initialization: $i = 0$, $k = 0$, $t_1 = 1$, $t_2 = L$, $\mathbf{y}_{M_1\times1} = \mathbf{0} + j\mathbf{0}, \mathbf{g}_{M_3\times1} = \mathbf{0} + j\mathbf{0}$.

repeat
  $i = i + 1$
  $\mathbf{x}_{M_1\times1} = \mathbb{DFT}\{\mathbf{b}_{r\{i,1\}}, M_1\}$
  $y_n = 2x_n^2 \ ; \ \forall\ n \in \left[2 \ \ \frac{M_1}{2}\right]$
  $y_n = x_n^2 \ ; \ n = \{1, \frac{M_1}{2} + 1\}$
  $\mathbf{u}_{M_1\times1} = \mathbb{IDFT}\{\mathbf{y}, M_1\}$
  $P_i^{\{1\}} = \mathbb{PCC}\{|\mathbf{u}|, \text{flipud}\{|\mathbf{u}|\}\}$
  if $P_i^{\{1\}} < P_{Th}^{\{1\}}$ **then**
    $t_2 = (i-1) \times m_1 + \frac{M_1}{2}$
    if $(t_2 - t_1) > T_{Th}$ **then**
      $k = k + 1$
      $\mathbf{f}_{M_2\times1} = \mathbb{DFT}\{\mathbf{b}_{r\{k,2\}}, M_2\}$
      $\hat{F}_k = \max(|f_n|) \ ; \ \forall\ n \in \ [1 \ \frac{M_2}{2}]$
      $t_1 = i \times m_1 - \frac{M_1}{4}$
    end if
  end if
until $(k \geq N_{DT}$ **or** $i \geq N)$
if $k = 0$ **then**
  $i = 0$
  $C = 1$
  repeat
    $i = i + 1$
    $\mathbf{h}_{M_3\times1} = \mathbb{DFT}\{\mathbf{b}_{r\{i,3\}}, M_3\}$
    $g_n = 2|h_n|^2 \ ; \ \forall\ n \in \left[2 \ \ \frac{M_3}{2}\right]$
    $g_n = |h_n|^2 \ ; \ n = \{1, \frac{M_3}{2} + 1\}$
    $\mathbf{v}_1 = \mathbb{IDFT}\{\mathbf{g}, M_3\}$
    $g_n = 2h_n^2 \ ; \ \forall\ n \in \left[2 \ \ \frac{M_3}{2}\right]$
    $g_n = h_n^2 \ ; \ n = \{1, \frac{M_3}{2} + 1\}$
    $\mathbf{v}_2 = \mathbb{IDFT}\{\mathbf{g}, M_3\}$
    $P_i^{\{2\}} = \mathbb{PCC}\{|\mathbf{v}_1|, |\mathbf{v}_2|\}$
    if $P_i^{\{2\}} < P_{Th}^{\{2\}}$ **then**
      $C = 3$
    end if
  until $(i \geq N_{CT}$ **or** $C = 3)$
else
  $\triangle\hat{F}_{\text{min}} = \min\{|\hat{F}_n - \hat{F}_{n-1}|\}; \ \forall\ n \in [2 \ \ k]$
  if $[\triangle\hat{F}_{\text{min}} < B_{Th}]$ **then**
    $C = 2$
  else
    $C = 4$
  end if
end if

Output: C.
Class Index (C): 1: Unmod, 2: PM, 3: FM & 4: FH

Nature of correlation loss with phase change & hop events is demonstrated. Fig. 3 shows the acquired IF plots for PM & FH cases over 500 MHz BW. Spectral stationarity of PM signals over chip duration & that of FH over sub pulses is shown.

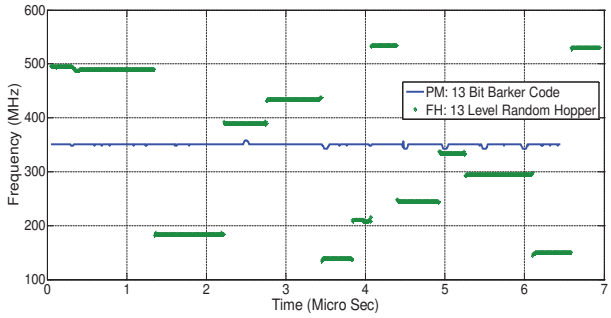

Fig. 3. Instantaneous frequency plots for 13-bit Barker coded & 13-level frequency hopper signals in intermediate frequency range at 4 dB SNR.

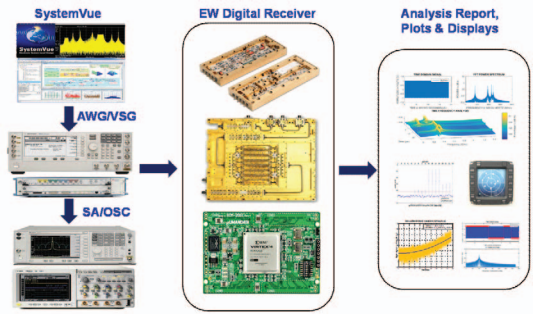

Fig. 4. Lab set up for intra-pulse analysis using SystemVue, AWG, VSG and EW digital receiver (*Image Courtesy*: M/s Keysight Technologies).

Practical EW DRx set up in laboratory to evaluate the algorithm is presented in Fig. 4. Test signals are generated using SystemVue radar library, in arbitrary waveform generator (AWG) at digital level and analog RF output is taken from vector signal generator (VSG). RF signals in the frequency range of radars were given as input to DRx, in injection mode, where it undergoes front end low noise processing, channelization, signal conditioning, down conversion, intermediate frequency processing, digitization and sample storing. Stored sample vectors are routed to the algorithm by system software and intra-pulse analysis report & plots are displayed as output.

VI. Performance Analysis

In this section, demonstration of intra-pulse classification and performance quantification of the algorithm is presented. A typical X-band, LFMCW radar signal with triangular IF structure, generated in the rig and analysed by intra-pulse analyzer is illustrated. Fig. 5 shows spectrum of the input signal. Analyzer performs pulse detection, extraction, modulation classification, parameter estimation and IF & signal reconstruction. Fig. 6 is the plot of reconstructed IF vector along with parameter estimates, true class and declared class.

Next, performance quantification over SNR by random MATLAB® trials is presented [15]. In each trial, input signal is designed by random selection of modulation class and signal parameters over the multi-parametric space, under uniform distribution. Thresholds and indices are set based on system design & processing considerations as discussed. Input vector

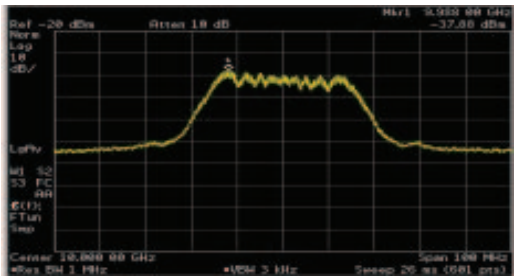

Fig. 5. LFMCW analysis demo: Spectrum analyzer display of input signal with, $F = 10$ GHz, $B = 32$ MHz, $\beta = 16\ \frac{\text{MHz}}{\mu\text{S}}$, $N_s = 6$.

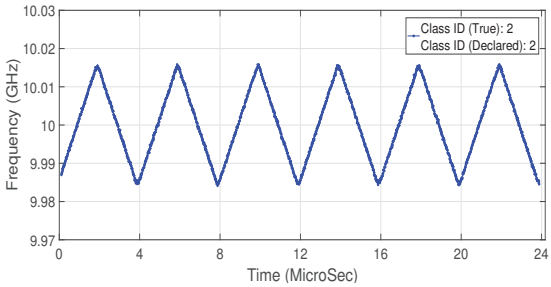

Fig. 6. LFMCW analysis demo: Reconstructed IF plot of test signal. $\hat{F} = 10.001$ GHz, $\hat{B} = 31.55$ MHz, $\hat{\beta} = 16.018\ \frac{\text{MHz}}{\mu\text{S}}$, $\hat{N}_s = 6$.

to the algorithm comprises one pulse of test signal. Parametric space for test signal generation is enumerated below.

- FM bandwidth: 5 MHz to 490 MHz
- FM slope: 5 $\frac{\text{MHz}}{\mu\text{S}}$ to 60 $\frac{\text{MHz}}{\mu\text{S}}$
- Barker code length: 2, 3, 4, 5, 7, 11 & 13 Bit
- Frank code length: 3×3 to 10×10
- PM chip width/FH sub pulse width: 200 nS to 2 μS
- FH resolution: 5 MHz (Min)
- Number of hops: 2–20
- Unmod pulse width: 400 nS to 20 μS
- Initial phase offset: $\sim \mathcal{U}[0\ \ 359]$ Deg
- SNR range for analysis: -3 dB to 9 dB, 1 dB step size
- Number of trials: 10 000 per SNR case.

Traditionally, confusion probability matrix (CPM) is used to quantify classification performance. However, considering that we have 13 CPMs, classification probabilities are presented in consolidated tabular form in Fig. 7. Each row corresponds to an SNR case, formed by stacking rows of 4×4 CPMs.

In Fig. 7, three SNR regions are distinct. In -3 to $+3$ dB region, DT FH classification is pre-dominant due to noise induced $P_{Th}^{\{1\}}$ crossings. Between 3 to 6 dB SNR, CT classification gradually improves and transition from unusable to stable classification region is observed. Above 6 dB SNR, CPMs are close to identity. In the stable region $\mathcal{P}_{11} = 1$ and $\mathcal{P}_{ii} \approx 1$ for $i > 1$. $\mathcal{P}_{24}$, $\mathcal{P}_{31}$, $\mathcal{P}_{34}$ and $\mathcal{P}_{43}$ are observed to be non-zero. MATLAB work space for each wrong classification case has been analyzed separately. $\mathcal{P}_{24}$ is controlled by B_{Th}. Increasing B_{Th} improves $\mathcal{P}_{24}$ at the cost of minimum hop size for FH. Also, all the $\mathcal{P}_{24}$ cases were observed for Barker

Probability → / SNR (dB) ↓	$\mathcal{P}_{11}$	$\mathcal{P}_{12}$	$\mathcal{P}_{13}$	$\mathcal{P}_{14}$	$\mathcal{P}_{21}$	$\mathcal{P}_{22}$	$\mathcal{P}_{23}$	$\mathcal{P}_{24}$	$\mathcal{P}_{31}$	$\mathcal{P}_{32}$	$\mathcal{P}_{33}$	$\mathcal{P}_{34}$	$\mathcal{P}_{41}$	$\mathcal{P}_{42}$	$\mathcal{P}_{43}$	$\mathcal{P}_{44}$
-3	0	0.9960	0	0.0040	0	0.8359	0	0.1641	0	0.0044	0	0.9956	0	0	0	1
-2	0	1	0	0	0	0.9622	0	0.0378	0	0.0044	0	0.9956	0	0	0	1
-1	0.0004	0.9996	0	0	0	0.9927	0	0.0073	0	0.0020	0	0.9980	0	0	0	1
0	0.0200	0.9800	0	0	0	0.9952	0	0.0048	0	0.0049	0	0.9951	0	0	0	1
1	0.1677	0.8323	0	0	0	0.9960	0	0.0040	0	0.0012	0.0236	0.9752	0	0	0	1
2	0.7087	0.2913	0	0	0	0.9988	0	0.0012	0.0004	0	0.1814	0.8181	0	0	0.0004	0.9996
3	0.9662	0.0338	0	0	0	0.9977	0	0.0023	0.0004	0	0.5738	0.4258	0	0	0.0008	0.9992
4	0.9973	0.0027	0	0	0	0.9988	0	0.0012	0.0008	0	0.8605	0.1387	0	0	0.0012	0.9988
5	1	0	0	0	0	0.9976	0	0.0024	0.0024	0	0.9667	0.0309	0	0	0.0004	0.9996
6	**1**	**0**	**0**	**0**	**0**	**0.9988**	**0**	**0.0012**	**0**	**0**	**0.9968**	**0.0032**	**0**	**0**	**0.0016**	**0.9984**
7	**1**	**0**	**0**	**0**	**0**	**0.9976**	**0**	**0.0024**	**0.0008**	**0**	**0.9988**	**0.0004**	**0**	**0**	**0.0012**	**0.9988**
8	**1**	**0**	**0**	**0**	**0**	**0.9980**	**0**	**0.0020**	**0**	**0**	**1**	**0**	**0**	**0**	**0.0024**	**0.9976**
9	**1**	**0**	**0**	**0**	**0**	**0.9988**	**0**	**0.0012**	**0.0008**	**0**	**0.9992**	**0**	**0**	**0**	**0.0021**	**0.9979**

Fig. 7. Classification performance summary: $i = 1, 2, 3$ & 4 correspond to Unmod, PM, FM & FH classes respectively. $\mathcal{P}_{ii}$ designator denote columns with probabilities of correct classification. $\mathcal{P}_{ik}$ denote probability of classification of ith class as kth class. Results are for 10 000 random trials per SNR case.

2-bit signals with chip width $<$ 230 nS. Next observation is on FM getting classified as Unmod or FH, i.e. $\mathcal{P}_{31}$ and $\mathcal{P}_{34}$. $\mathcal{P}_{31}$ c1ases were seen for some cases of FM signals with BW $<$ 6 MHz, while $\mathcal{P}_{34}$ were observed for FM slopes $> 54\ \frac{\text{MHz}}{\mu\text{S}}$. Such steep FM slopes are interpreted as hopping. This shows that current method has non zero $\mathcal{P}_{ii}$ in handling FM BW $<$ 6 MHz and slopes $> 54\ \frac{\text{MHz}}{\mu\text{S}}$. Decreasing $P_{Th}^{\{1\}}$ improves $\mathcal{P}_{34}$ and the associated penalty is minimum phase change and FH size, which the classifier can handle. $\mathcal{P}_{43}$ is due to some of the 2-level FH SOIs with hop size $<$ 7 MHz failing to cross $P_{Th}^{\{1\}}$ level. Summarizing, it is observed that most of the wrong classifications have occured for signals with parametric extremes like least hop size, least BW, narrow PW etc. *Intentionally*, parametric boundaries for performance analysis have been kept beyond the achievable bounds with the proposed method, to demonstrate performance in the valid region and nature/quantum of degradation near boundaries.

VII. Conclusion

Current work addresses the prominent problem of threat radar signal classification and scenario cognition in EW receivers. Underlying frequency and phase structure of each modulation class and its response to specific signal processing functions have been used as criterions for classification. No apriori knowledge of modulation structures are assumed and classification is solely based on the CT or DT process embedded in the SOI. Applicability of the proposed method to any arbitrary signal structure is of practical significance, since EW systems operate in a non-cooperative environment. System engineering approach has been adopted in choice of methods, their implementation and overall analysis architecture. It may be observed that most of the signal processing functions, which are defined in time-domain, have been implemented in spectral domain, to harness the available transform cores in system firmware and software. Operationally, this leads to improved response time and resource utilization. Nature and quantum of degradation in performance near parametric limits has been discussed, while stable performance in the valid region has been demonstrated both in simulations and practical system. Laboratory rig facility to generate pulse compressed radar signals and implementation of algorithm in practical EW DRx is presented. Observed performance in the rig has been verified to be in agreement with the simulation studies and the quantified confusion probability matrices.

References

[1] Merrill. L. Skolnik, *Introduction to radar systems*, 3rd ed., Tata Mcgraw Hill Publications, 2001.

[2] Philip. E. Pace, *Detecting and classifying low probability of intercept radar*, Artech House Inc, 2004.

[3] Product Datasheet, M/s Thales Group, *VIGILE Advanced Naval R-ESM/ELINT Systems*, www.thalesgroup.com, 2012.

[4] Product Datasheet, M/s Selex ES, *SAGE Advanced Digital ESM*, www.selex-es.com, 2014.

[5] Product Datasheet, M/s Saabgroup, *SIRIUS Airborne SigInt System*, www.saabgroup.com.

[6] Product Datasheet, M/s Rockwell Collins, *CS3045 Airborne ELINT/ESM Subsystem*, www.rockwellcollins.com, 2009.

[7] J. Lunden and V. Koivunen, "Automatic radar waveform recognition," *IEEE Journal on Sel. Topics in Sig. Proc.*, 2007, vol. 1, no. 1, pp. 124–136.

[8] J. Terho Lunden and L. Koivunen, V, "Classifying pulse compression radar waveforms using time frequency distributions," in *Conference on Info Sciences and Systems*, The Johns Hopkins University, Mar. 2005.

[9] Brandon Hamschin, John Clancy, Mike Grabbe, Matthew Fortier, and John Novak, "Passive detection, characterization, and localization of multiple LFMCW LPI signals," *IEEE RadarCon*, 2014, pp. 537–543.

[10] J. Rossouw van der Merwe, Warren P. du Plessis, Francois D. V. Maasdorp, and J. E. Cilliers, "Introduction to low probability of recognition to radar system classification," *IEEE RadarCon*, 2016, pp. 1–5.

[11] Pei Wang, Zhaoyang Qui, Jun Zhu, and Bin Tang, "Autonomous radar pulse modulation classification using modulation component analysis," *EURASIP Journal on Advances in Signal Processing*, Sep. 2016, DOI:10.1186/s13634-016-0394-3.

[12] Zhutian Yang, Wei Qiu, Hongjian Sun, and Arumugam Nallanathan, "Robust radar emitter recognition based on the three-dimensional distribution feature and transfer learning," *Sensors*, 2016, vol. 16, no. 3, DOI: 10.3390/s16030289.

[13] Zhaoyang Qiu, Pei Wang, Jun Zhu, and Bin Tang, "A parameter estimation algorithm for LFM/BPSK hybrid modulated signal intercepted by Nyquist folding receiver," *EURASIP Journal on Advances in Signal Processing*, Aug. 2016, DOI: 10.1186/s13634-016-0387-2.

[14] Leon Cohen, *Time-frequency analysis*, Prentice Hall, 1995.

[15] MATLAB 2016b, Version No: 9.1.0.441655, License No:1070594, M/s Mathworks Inc, 2016.